

Optimization of a Microfluidic Chip Using Capillary Pumps and Stop Valves for Target Screening

Junjie Hong¹, Silu Feng^{1*}

¹School of Integrated Circuits, Guangdong University of Technology

Abstract

This study introduces a novel microfluidic chip that integrates biosensors, capillary pumps, and stop valves, aimed at enhancing target screening and fluid control precision. We detail the fluid control mechanism's theoretical framework, establishing the chip's operation within laminar flow parameters through preliminary calculations. Utilizing COMSOL Multiphysics, we simulate the microfluidic model, outlining critical settings for initialization and boundary conditions, thus validating our fluid control approach. Notably, we present a "bone-like" structural enhancement to the capillary pump channel, which reduced liquid filling time from 1.85 seconds to 1.5 seconds, achieving an 18% improvement. These findings offer insights for optimizing capillary pump designs, ultimately advancing the efficiency of microfluidic liquid delivery and enhancing lab-on-a-chip applications.

Keywords: Fluid mechanics, Capillary pump, Multiphysics Simulation

Introduction

Rapid and accurate sample analysis is crucial for the early diagnosis and treatment of diseases in modern medical research and clinical diagnosis. Traditional laboratory analysis methods often require complex equipment, professionals, and a long period of time, which is inadequate in resource-limited environments or when rapid field response is required. Microfluidic chip technology provides a miniaturized, integrated fluid control solution capable of operating independently under these conditions.

This paper introduces a novel microfluidic chip equipped with biosensors and integrated capillary microfluidics, designed for target screening and precise fluid control. The chip's capillary pumps enable spontaneous fluid delivery to the sensors without the need for external pumps, while the stop valve regulates flow, ensuring reliable operation in field settings or resource-limited environments^[1]. The sensor array can be functionalized with different biosensors specific to various targets, making the chip capable of screening and identifying targets in unknown samples^[2]. By integrating different functions on a microfluidic chip, the operations of sample transmission, rapid response, accurate detection and timely cleaning are automatically completed on the chip, thus greatly improving the analysis efficiency^[3]. However, the functionality of microfluidic chips is closely related to the design of capillary pumps, contact angle (wettability), stop valves, as well as the liquid's surface tension and viscosity. Even minor variations in these parameters can significantly impact the performance of the microfluidic system^[4]. As a result, designers often need to verify whether their designs function as intended or meet the desired specifications. Computational fluid dynamics (CFD) simulations

offer a valuable tool for design validation, enabling designers to test their concepts virtually, thereby saving time and reducing manufacturing costs^[5]. In this study, the CFD module within COMSOL Multiphysics is employed to model a microfluidic chip incorporating capillary pumps and stop valves. Through numerical simulation and analysis of fluid dynamics within the microchannels, as well as the regulation of stop valve functionality, the performance of the capillary pump is validated. Additionally, the internal structure and dimensions of the chip are optimized based on simulation results.

Theory

The flow state of a fluid can be characterized by the Reynolds number, a dimensionless parameter that expresses the ratio of inertial forces to viscous forces in a fluid system. It serves as a critical criterion for predicting different flow regimes. When $Re < 2000$, the fluid typically exhibits laminar flow, where the motion is orderly and smooth. In the range $2000 < Re < 4000$, the flow enters a transitional phase, characterized by instability and the potential for chaotic behavior. For $Re > 4000$, the flow becomes turbulent, marked by irregular fluctuations and mixing. In case where the Reynolds number is significantly less than 1 ($Re \ll 1$), the flow is classified as creeping or Stokes flow, where viscous forces dominate. In this study, preliminary calculations yield a Reynolds number of approximately 10, situating the flow firmly within the laminar regime, where viscous forces maintain smooth fluid motion.

Reynolds number :

$$Re = \frac{\rho \times u \times D}{\mu}$$

In the above formula, ρ is the fluid density, u is the fluid velocity, D channel size or diameter, and μ is the dynamical viscosity of the fluid.

Fluid mechanics has three fundamental physical laws: the conservation of mass, Newton's second law, and the conservation of energy. These principles are mathematically expressed through the Navier-Stokes equations and the continuity equation^[6]. Under microscale conditions, an aqueous solution can be approximated as an incompressible, viscous fluid. In such a system, if no external forces are acting on the liquid and the temperature remains constant, the fluid flow is typically characterized as laminar. Under these assumptions, the liquid can be described by the following simplified equations:

continuity equation :

$$\frac{\partial \rho}{\partial t} + \nabla(\rho \cdot \mathbf{V}) = 0$$

Navier-Stoke equation is divided into

Equation of mass conservation:

$$\nabla \cdot \mathbf{V} = 0$$

and Equation of momentum conservation:

$$\frac{\partial \mathbf{p}}{\partial t} + (\mathbf{u} \cdot \nabla)\mathbf{u} = -\frac{\nabla \mathbf{p}}{\rho} + \frac{\mu \nabla^2 \mathbf{u}}{\rho}$$

In the above three equations, V is the volume of the liquid, the fluid density entering the microfluidic chip, u is the velocity vector of the fluid, p is the channel pressure of the fluid to the microfluidic chip, μ is the dynamic viscosity of the fluid, ∇ it is the gradient operator, and ∇^2 is the Laplacian operator.

The stop valve operates based on the capillary-driven flow, which arises from surface tension effects. This phenomenon is governed by the Laplace and Young's equations. The Laplace equation describes the relationship between the pressure difference across the liquid interface and its curvature. The Young's equation explains the balance of interfacial tension between liquids, solids, and gases.

Laplace's equation:

$$\Delta P = \gamma \left(\frac{1}{R_1} + \frac{1}{R_2} \right)$$

ΔP is the pressure difference inside and outside of the liquid, γ is the liquid surface tension, R_1 and R_2 is the main radius of curvature of the liquid interface. The equation shows that the greater the liquid surface curvature, the greater the pressure difference needed to overcome.

Yang's equation:

$$\gamma_{ls} + \gamma_{lg} \cos\theta = \gamma_{gs}$$

γ_{gs} is the solid-gas interfacial tension, γ_{ls} is the solid-liquid interfacial tension, γ_{lg} is the liquid-gas interfacial tension, and θ is the contact angle of the liquid on a solid surface. This equation shows that

the contact angle affects the wettability of the liquid and determines how the liquid flows on a solid surface.

Modeling

We used AUTOCAD to design the microfluidic chip, which consists of the following components from left to right: a lateral capillary pump on the left, a biosensor module, stop valves, and a longitudinal capillary pump on the right. Key parameters are provided in Table.1, and the corresponding microfluidic chip model is illustrated in Figure .1 below.

Parameter	Value
Capillary channel size	0.4 mm
Detection area size	2*2 mm
Detection area channel size	1 mm
Stop valve channel size	0.3 mm
Microfluidic chip size	53*23 mm

Table 1. Microfluidic chip modeling section size parameters

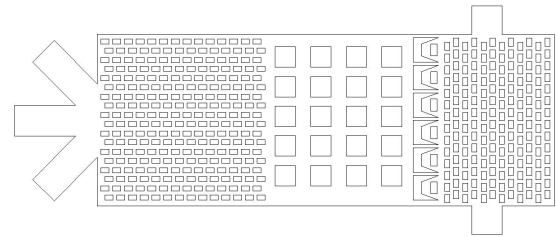


Figure 1. Microfluidic chip model

Simulation

In this study, the CFD module within COMSOL Multiphysics was utilized to simulate the fluid dynamics in the microfluidic chip. The Multiphase Flow interface was selected, specifically the Two-Phase Flow^[7], Phase Field method, in conjunction with the Laminar Flow and Transient options for phase initialization. The microfluidic chip model, designed in AutoCAD, was imported into the geometry module of the software for further analysis.

To simulate the spontaneous capillary filling process, water and air were assigned as the working fluids. Boundary conditions were applied by defining inlets and outlets within the laminar flow setup. Since the fluid droplets naturally progress from the inlet toward the sensor region, the boundary conditions at the inlet and outlet were pressure-based, with static pressure specified at both points.

In the Phase Field interface, the inlet was set to represent Fluid 2 (water), and the wetting angle was specified along the wetting walls. Initial phase field

values were assigned, ensuring the Fluid 2 (water) was designed as the inlet variable. A free triangular mesh was generated for the model, and mesh refinement was set to Hyperrefinement to enhance simulation accuracy. The final step involved defining the time step and simulation duration, after which the software proceeded with automatic mesh generation and the execution of the simulation.

Parameter	Value
static pressure	0 Pa
wettability angle of the capillary pump	75 Deg
Wettability angle of the stop valve	150 Deg
Interface thickness parameters	0.002
step size	0.005
stop time	15 s

Table 2. Simulation to set the relevant parameters

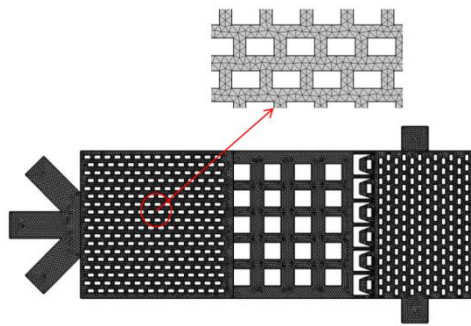


Figure 2. Macro and micro mesh structure of the microfluidic chip

Result

Upon completion of the simulation, the spontaneous filling of the microfluidic chip by the liquid and the subsequent flow cessation due to the stop valve were observed. The volume fraction of the fluids is depicted in the figure 3, where the blue region represents Fluid 2(water), and the red region represents Fluid 1 (air).

At the initial time step (0s), as shown in Figure 3(a), the liquid enters the microfluidic chip from the inlet. The flow velocity increases as the liquid passes through the capillary pump, where the flow rate stabilizes. At around 0.1s(Figure 3b), the liquid has flowed to about halfway through the capillary pump. By approximately 0.2s (Figure 3c), the liquid fully infiltrates the capillary pump, and upon reaching the biosensor area, the flow rate begins to decelerate. At 1.5 seconds (Figure 3d), liquid is slowly filling the biosensor module. At around 1.85s (Figure 3e), the liquid has completely filled both the left-side capillary pump and the biosensor module. Throughout the 15s simulation period (Figure 3f), the stop valve effectively prevents the

liquid from overflowing, confining the liquid to the left-side region.

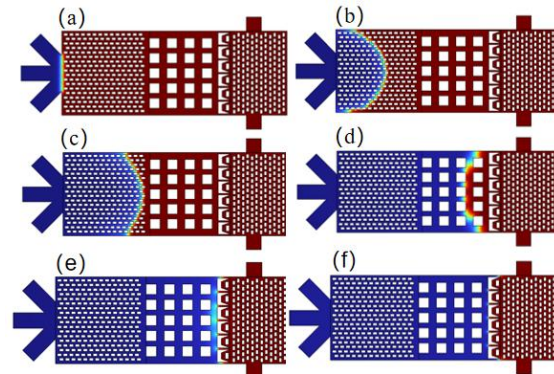


Figure 3. Microfluidic chip simulation. Image of volume fraction in each time period, figure (a) is the image at 0s, figure (b) is the image at 0.1s, figure (c) is the image at 0.2s, figure (d) is the image at 1.5s, figure (e) is the image at 1.85s, and figure (f) is the image at 15s.

Discussion

In this latest simulation study, we introduced improvements to the capillary pump channel structure by replacing the conventional square-channel design with a novel "bone-like" structure, as illustrated in the accompanying microscopic images^[8]. This "bone-like" structure, due to its more intricate geometry, required approximately ten times the number of mesh elements compared to the square-channel structure, resulting in a significantly longer simulation time.

To assess the impact of this structural modification on fluid dynamics, we conducted a comparative analysis of liquid flow behavior between the two designs, while maintaining similar overall channel sizes (despite the irregularity introduced by the "bone-like" structure) and keeping other parameters constant. The results showed that the square channel structure required approximately 0.2 seconds(Figure 4a) for the liquid to pass through the capillary pump, whereas the "bone-like" structure achieved this in 0.185 seconds(Figure 4b), indicating a marginal improvement in flow speed. However, the differences became more pronounced when the liquid reached the biosensor area. The square-channel design required 1.85 seconds(Figure 4c) to fully fill the biosensor region, while the "bone-like" structure reduced this time to 1.5 seconds(Figure 4d).

These preliminary findings are promising, as they suggest that the "bone-like" channel design could offer notable advantages in terms of fluid transport efficiency. The reduction in filling time indicates improved flow dynamics, which may translate into more efficient operation of capillary pumps in microfluidic systems. The complex geometry of the "bone-like" structure appears to enhance fluid distribution and flow stability, even though the simulation time and computational resources required are significantly higher.

This study provides valuable insights into the potential of optimizing microchannel designs for

capillary-driven systems. While the improvements in flow speed are modest in the initial phase, the enhanced performance in the biosensor region highlights the potential of this design for more efficient liquid delivery. Future work will focus on further refining this structure to achieve even higher efficiency and better performance, particularly in applications requiring precise and rapid fluid control within microfluidic devices.

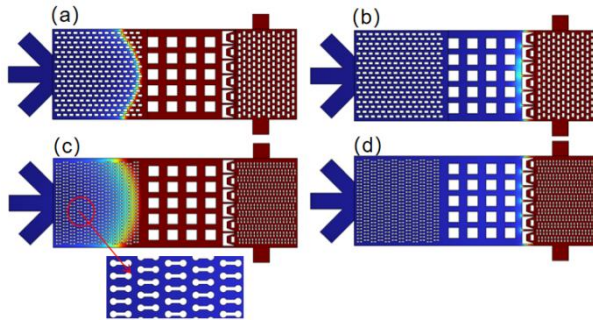


Figure 4. Figure (4a) is the image of the square structure at 0.2s. Figure (4b) is the image of the square structure at 1.85s. Figure (4c) is the image of the "bone-like" structure at 0.185s. Figure (4d) is the image of the "bone-like" structure at 1.5s. The "bone-like" capillary pump can be seen with faster pumping speeds.

Conclusion

Through comprehensive numerical simulations and analyses of fluid flow, solution mixing, and stop valve control within the microchannels, we successfully validated the functionality of the capillary pump in autonomously transporting liquid to the biosensor module. Additionally, the stop-valve effectively controlled liquid flow, ensuring precise regulation throughout the microfluidic chip. The simulation results demonstrated that the flow characteristics of the liquid droplets after passing through the microfluidic chip are strongly influenced by the dimensions of the capillary array and the wettability of the pump walls.

Moreover, we introduced a significant improvement to capillary pump by replacing the conventional square channel structure with a novel "bone-like" design. Although this new structure increased the simulation time by more than tenfold due to its geometric complexity, it also led to noticeable improvements in fluid velocity within the channels. Specifically, in the biosensor region, the "bone-like" structure reduced the liquid filling time from 1.85 seconds to 1.5 seconds, representing an 18% reduction. This enhancement underscores the potential of this innovative design for optimizing capillary pump performance.

These findings provide a valuable reference for further optimization and refinement of capillary pump designs in microfluidic systems. By leveraging such structural improvements, we anticipate further advancements in the efficiency of microfluidic liquid delivery, paving the way for

more effective and responsive lab-on-a-chip applications in the future.

Reference

- [1] Song, Y., Zhou, Y., Zhang, K., Fan, Z., Zhang, F., & Wei, M. (2024). Microfluidic programmable strategies for channels and flow. *Lab on a Chip*.
- [2] Kulkarni, M. B., Ayachit, N. H., & Aminabhavi, T. M. (2022). Biosensors and microfluidic biosensors: from fabrication to application. *Biosensors*, 12(7), 543.
- [3] Yang, S. M., Lv, S., Zhang, W., & Cui, Y. (2022). Microfluidic point-of-care (POC) devices in early diagnosis: A review of opportunities and challenges. *Sensors*, 22(4), 1620.
- [4] Haeberle, S., & Zengerle, R. (2007). Microfluidic platforms for lab-on-a-chip applications. *Lab on a Chip*, 7(9), 1094-1110.
- [5] P. Ebner and R. Wille, "CFD for Microfluidics: A Workflow for Setting Up the Simulation of Microfluidic Devices," 2023 26th Euromicro Conference on Digital System Design (DSD), Golem, Albania, 2023, pp. 770-775
- [6] Pishkoo, A., & Darus, M. (2021). Using fractal calculus to solve fractal Navier–Stokes equations, and simulation of laminar static mixing in COMSOL multiphysics. *Fractal and Fractional*, 5(1), 16.
- [7] Savola, A. (2012). Fluid flow modeling inside heat collection pipes with finite element method.
- [8] Z. Wu, X. Wang, M. Xu and L. Liu, "A fully capillary-driven μ DMFC twin-stack operating in all orientations," 2015 Transducers - 2015 18th International Conference on Solid-State Sensors, Actuators and Microsystems (TRANSDUCERS), Anchorage, AK, USA, 2015, pp. 934-937

Acknowledgment

National Natural Science Foundation of China (Grant No.32102078) to Silu Feng. Guangzhou Municipal Science and Technology (Project 2023A04J0351) to Silu Feng.
License:9421310